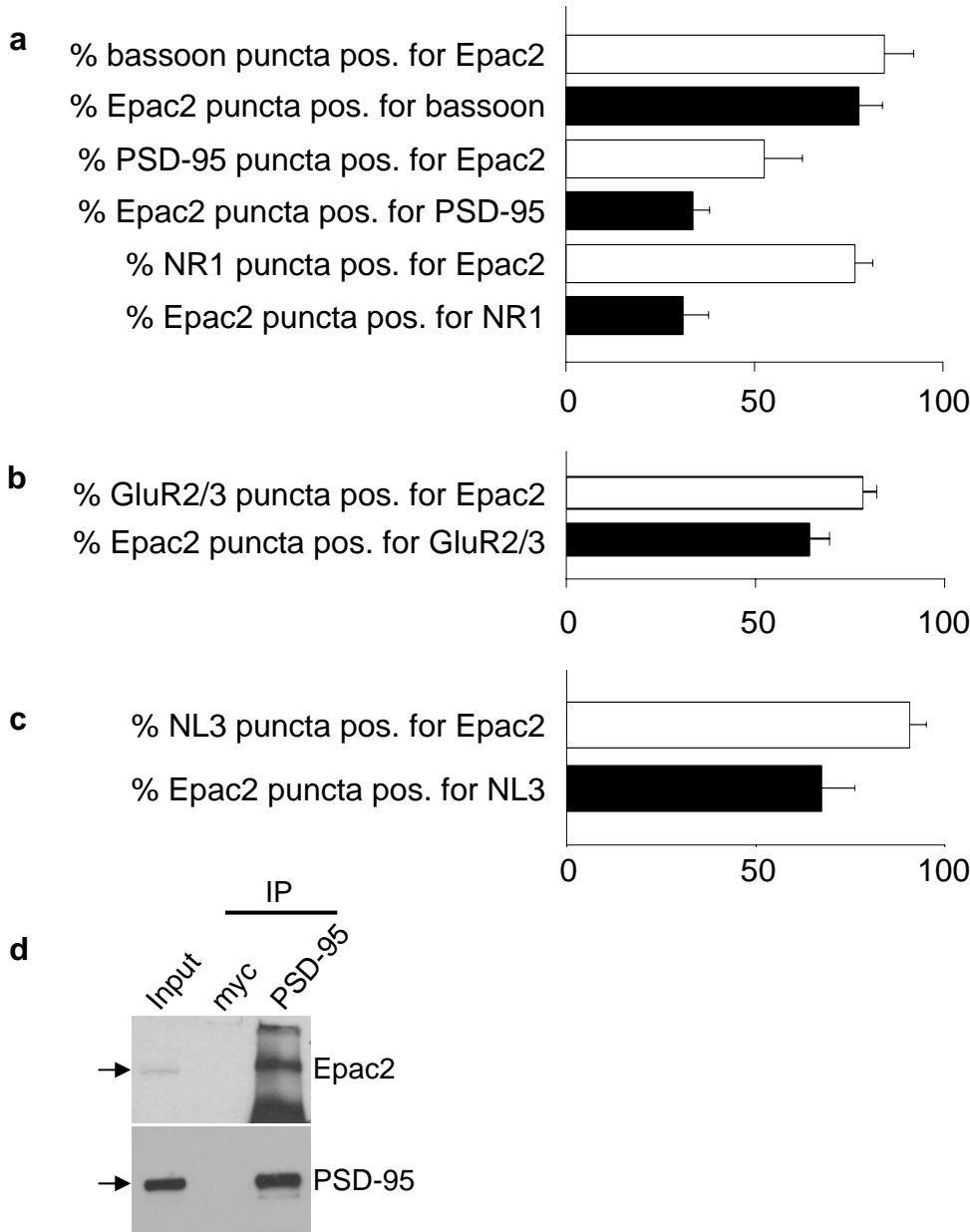
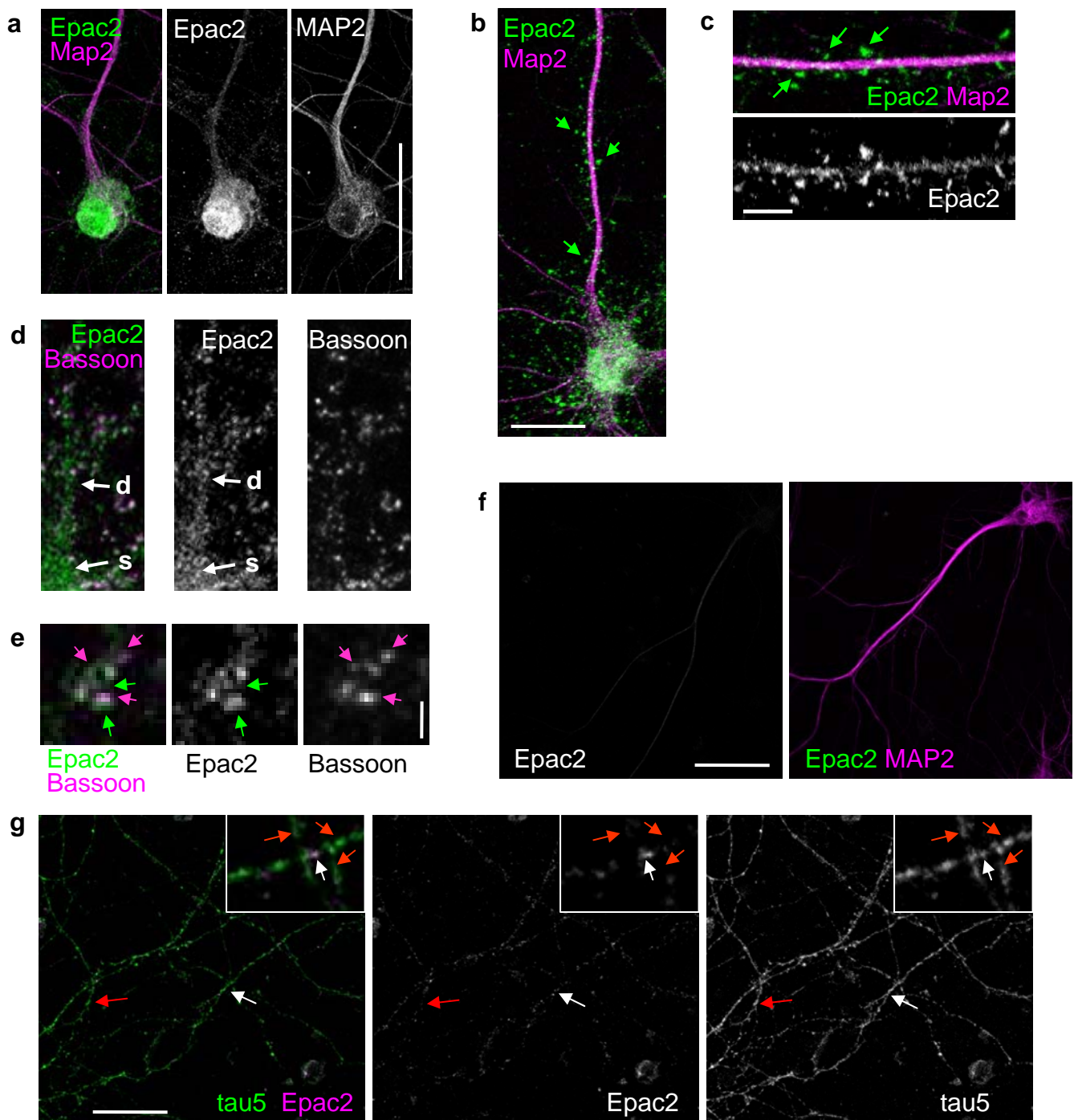


Epac2 induces synapse remodeling and depression and its disease-associated forms alter spine morphology

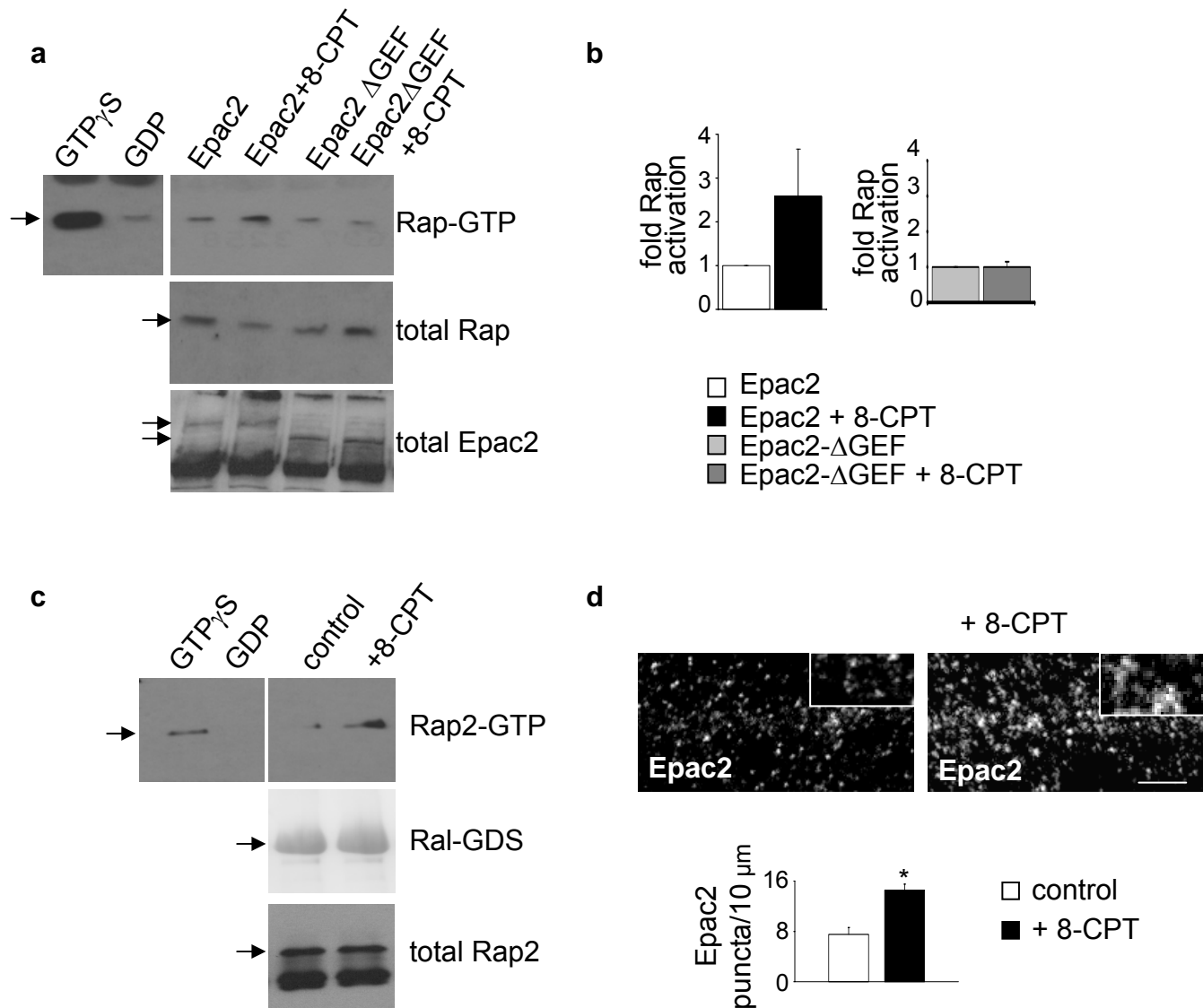
Kevin M. Woolfrey, Deepak P. Srivastava, Huzefa Photowala, Megumi Yamashita, Maria V. Barbolina, Michael E. Cahill¹, Zhong Xie, Kelly A. Jones, Lawrence A. Quilliam, Murali Prakriya, Peter Penzes



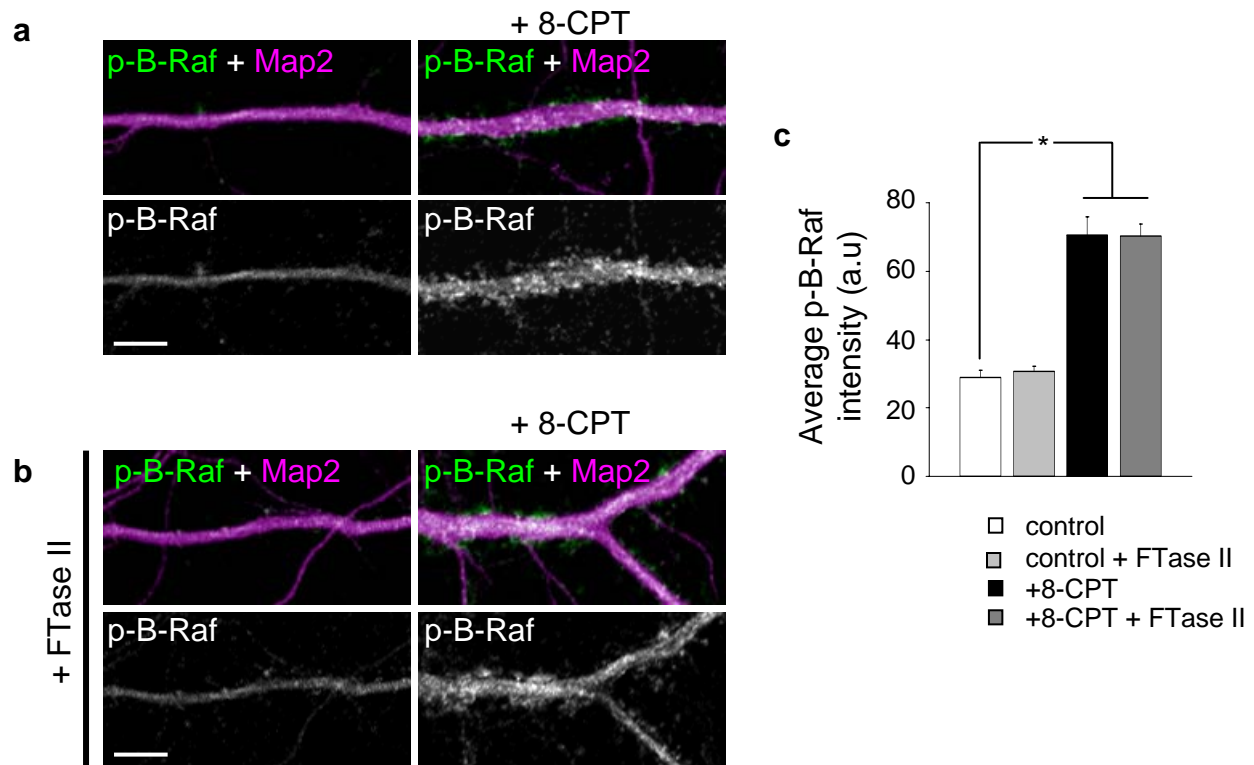
Supplementary Figure 1 Quantification of Epac2 immunofluorescence colocalization with synaptic proteins in dendrites. **(a)** Quantification of the reciprocal colocalization of Epac2 with bassoon, PSD-95, or NR1 in dendrites. **(b)** Quantification of the reciprocal colocalization of Epac2 with GluR2/3 in dendrites. **(c)** Quantification of the reciprocal colocalization of Epac2 with NL3 in dendrites. In all graphs, average intensities of overlapping signals were plotted, $n = 6-12$ cells, 1-3 experiments. **(d)** Coimmunoprecipitation of Epac2 with PSD-95 from rat forebrain; myc, control antibody.



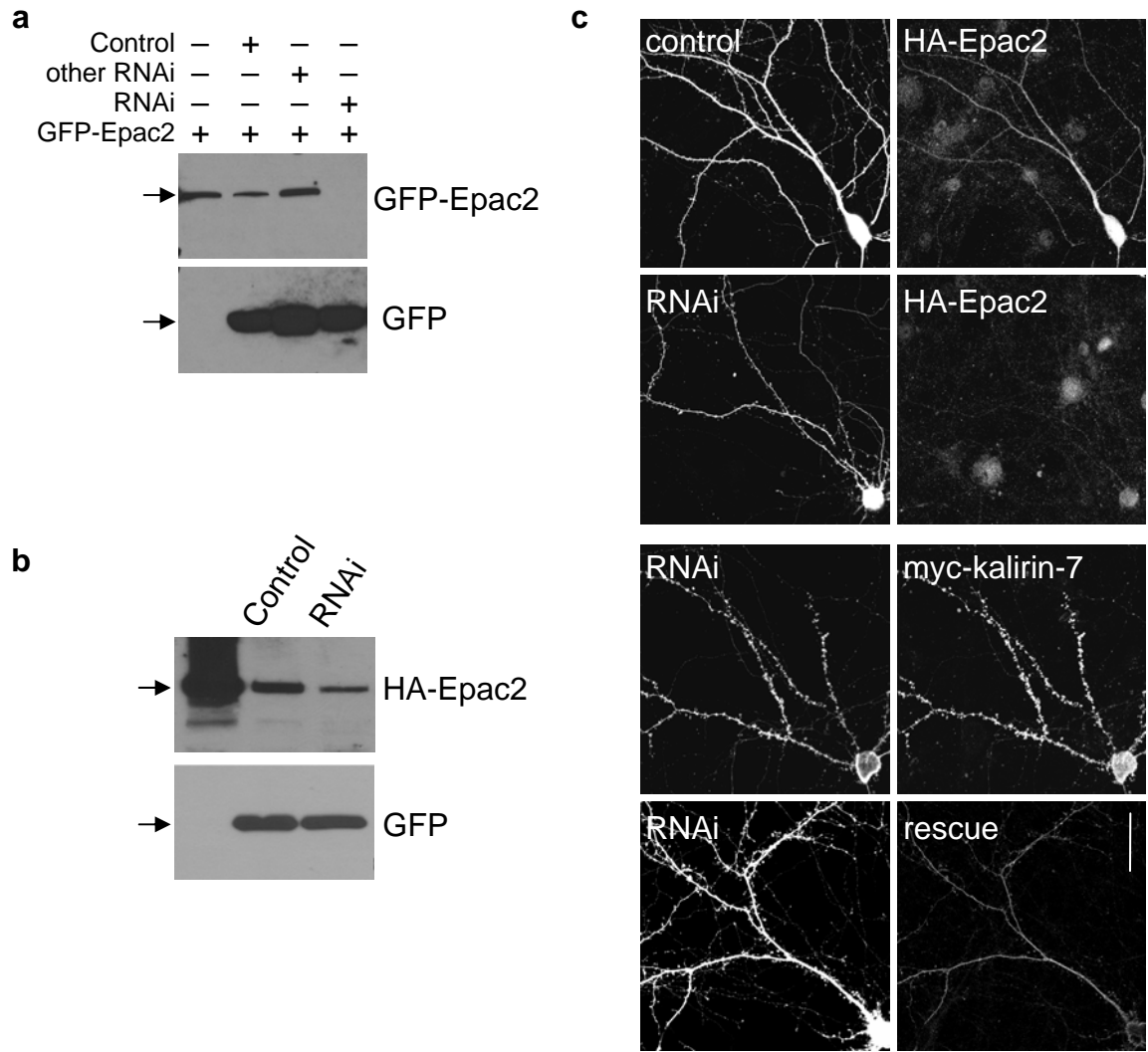
Supplementary Figure 2 Subcellular localization of Epac2 in pyramidal neurons. **(a)** Epac2 is detected in dendrites, as visualized by colocalization with the dendritic marker Map2. **(b-c)** Higher magnification images of Epac2 and Map2 immunofluorescence in dendrites. Arrows point to Epac2 clusters offset from the dendrite shaft. **(d)** Epac2 is present in the dendritic shaft (“d”) and soma (“s”). **(e)** Incomplete overlap between Epac2 and the presynaptic active zone marker bassoon. Purple arrows: bassoon only puncta; green arrows: Epac2-only puncta. **(f)** Lack of nonspecific detection of Epac2 by the secondary antibody, as shown by control lacking primary antibody. **(g)** Double immunofluorescent imaging of Epac2 and axonal marker tau. Insets: higher magnification images. Small puncta of Epac2 signal were also detected in axons. White arrows: Epac2 colocalized with tau; red arrows: tau signal without Epac2. Scale bars, a 35µm; b 15µm; c, d 5µm; e, 2.5µm; f, g, 15 µm.



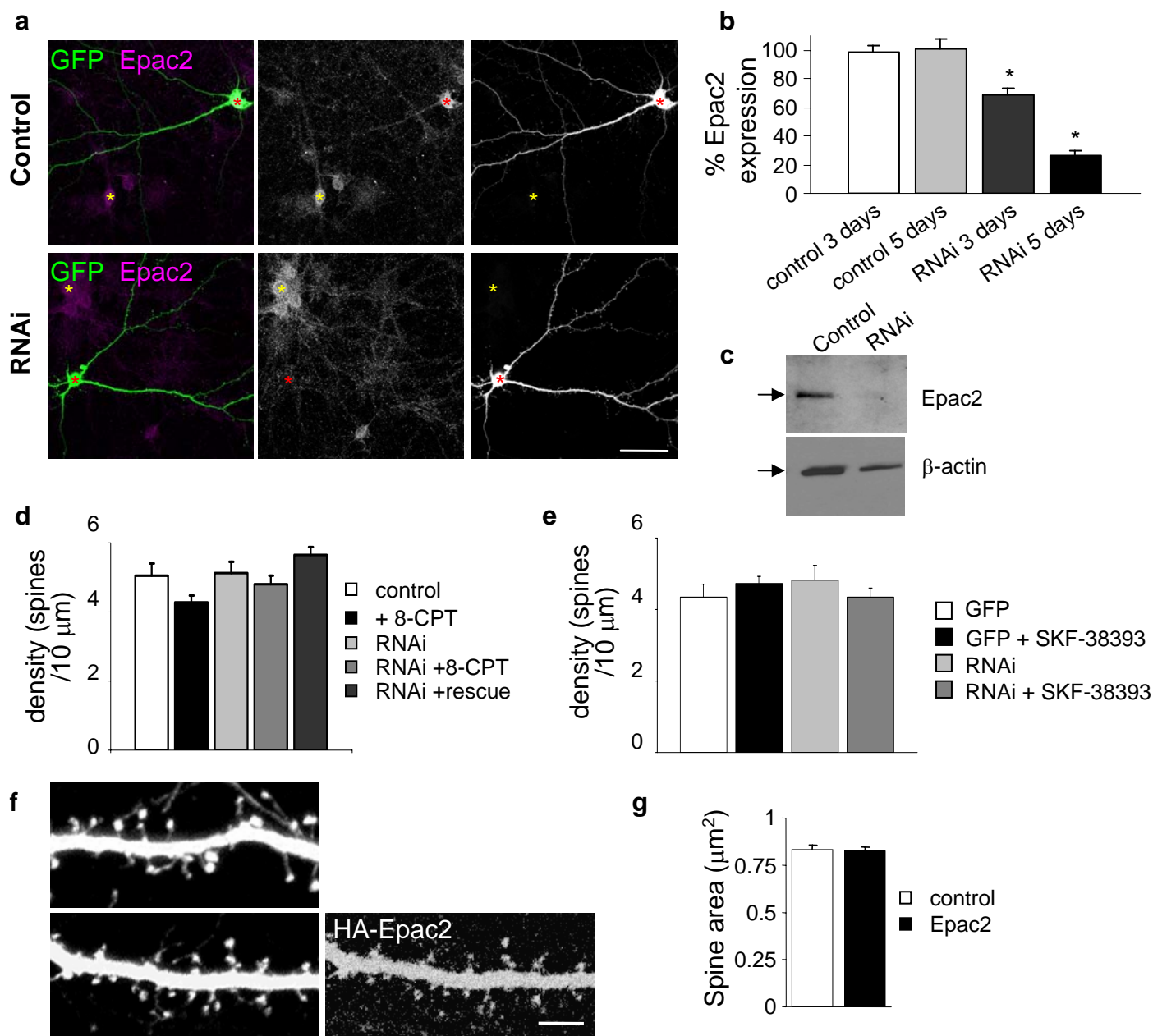
Supplementary Figure 3 Enhancement of Epac2 Rap-GEF activity by the Epac2-specific cAMP analog 8-CPT and effect on dendritic spine morphology. **(a)** Activation of Rap in presence of exogenous Epac2 by specific agonist 8-CPT depends on a functional GEF domain of Epac2. HEK293 cells were transfected with full-length HA-Epac2 or C-terminally truncated HA-Epac2-GEF lacking the Rap-GEF domain. Cells were treated with 8-CPT (10 μ M, 30 min) or left untreated, and activation of endogenous Rap1 was measured using a Rap activation assay kit. **(b)** Quantification of Rap1 activation by Epac2. Activation of Epac2 by 8-CPT is abolished by deletion of its Rap-GEF domain, $n = 4$ experiments, Western blot shows representative results. **(c)** Incubation of neurons with 8-CPT also activates Rap2, $n = 3$, Western blot shows representative results. **(d)** Incubation with 8-CPT (10 μ M), enhanced Epac2 dendritic clustering, $n = 8-12$ cells, 3 experiments.



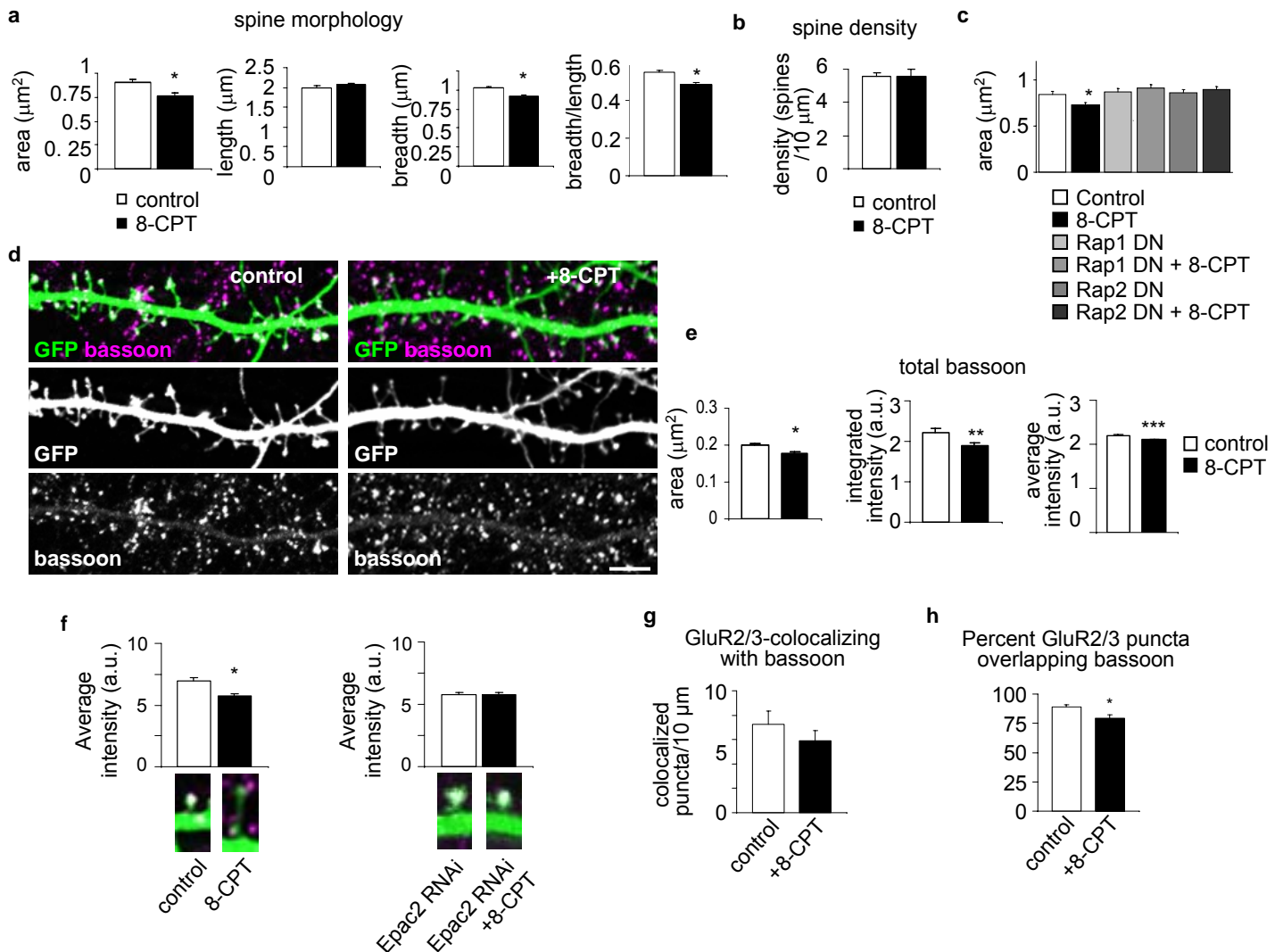
Supplementary Figure 4 Phosphorylation of B-Raf upon 8-CPT treatment is not Ras-dependent. **(a)** Effect of incubation with 8-CPT (50 μ M, 1 hr) on B-Raf phosphorylation *in situ* in pyramidal neuronal dendrites. Map2 immunofluorescence was used to outline dendrites. **(b)** Lack of effect of Ras inhibitor FTase II (200 μ M) on 8-CPT-dependent B-Raf phosphorylation in dendrites. **(c)** Quantification of B-Raf fluorescence intensities in a-b, $n = 8$ cells from 2 experiments.



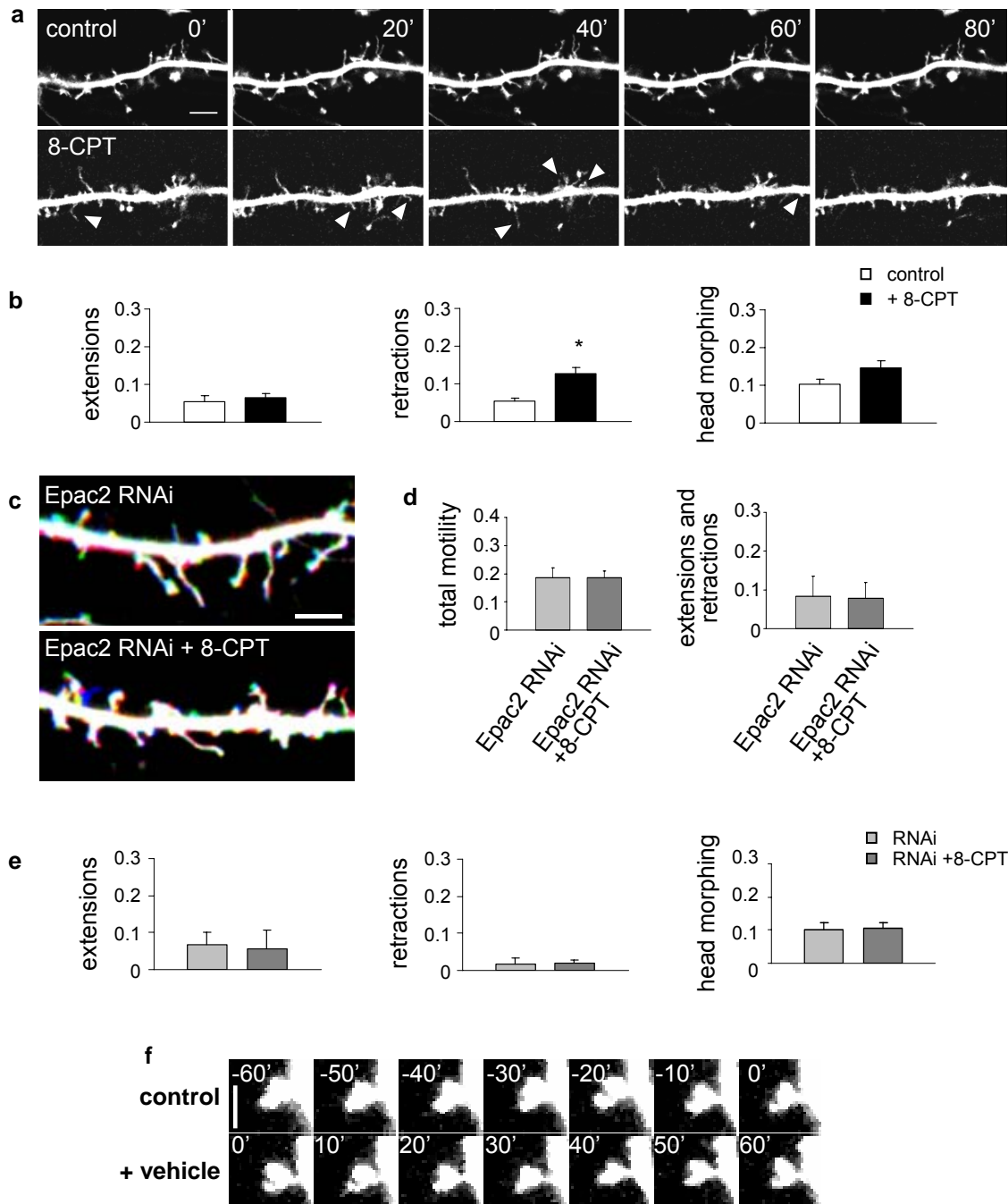
Supplementary Figure 5 RNAi-mediated knockdown of Epac2. **(a)** In hEK293 cells, expression of exogenous GFP-Epac2 is blocked by Epac2-specific RNAi, but not by control plasmid or RNAi targeting an unrelated mRNA; expression of all pGsuper plasmids was similar, as shown by expression of GFP. **(b)** RNAi-resistant mutant Epac2 expresses in the presence of Epac2-specific RNAi and control plasmid in hEK293 cells. **(c)** In cortical neurons, Epac2 RNAi specifically knocks down exogenous HA-Epac2 but not myc-kalirin expression; a control plasmid does not affect HA-Epac2 expression. A rescue plasmid encoding an RNAi-resistant mutant Epac2 expresses well. Scale bar, 35µm.



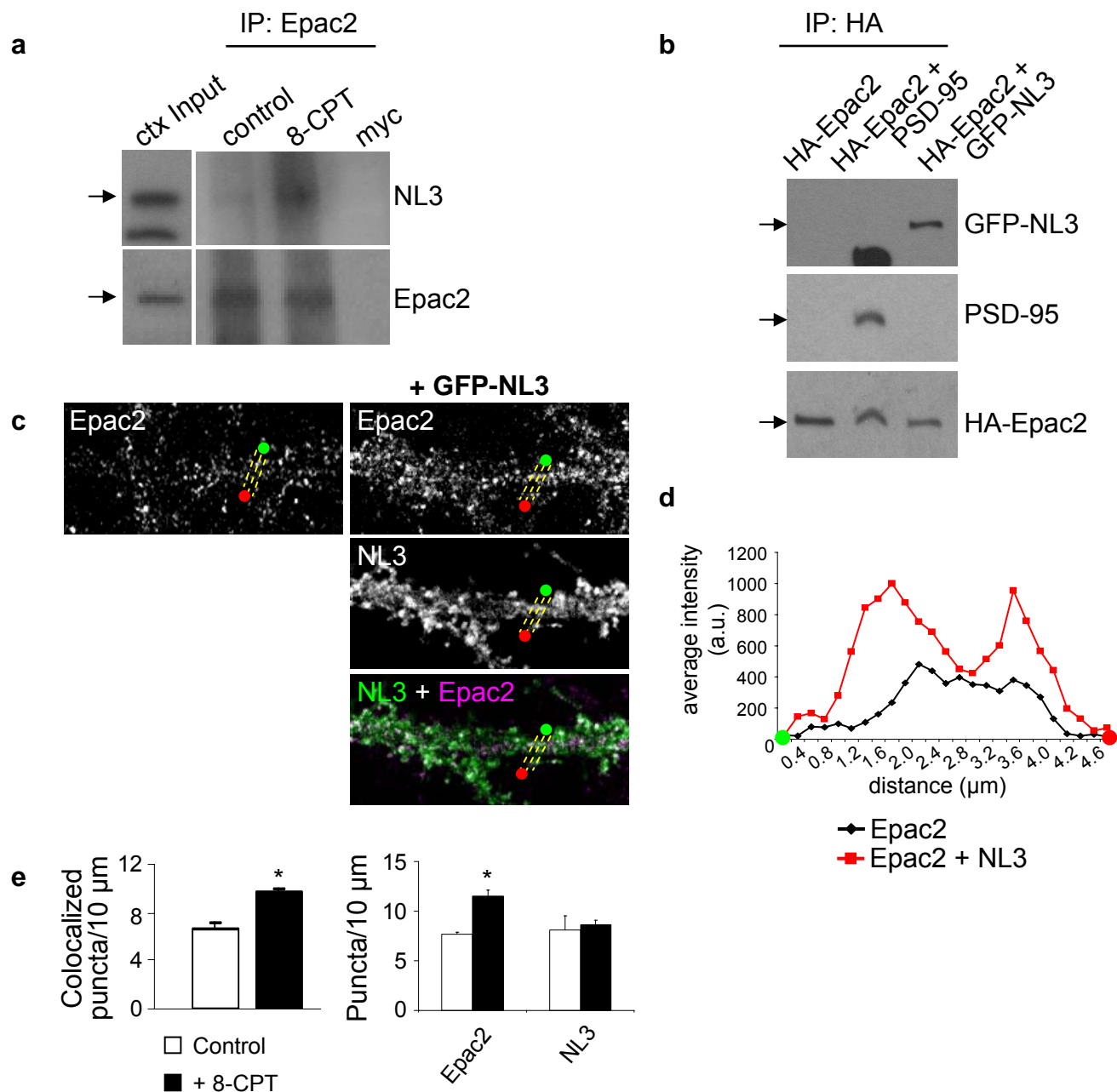
Supplementary Figure 6 RNAi-mediated knockdown of endogenous Epac2 in neurons. **(a)** Endogenous Epac2 is knocked down in cortical neurons transfected with Epac2-RNAi (red *), but not in neighboring non-transfected cells (yellow *). The GFP expressing cells are also expressing Epac2-RNAi. RNAi was expressed for 3 or 5 days. **(b)** Quantification of Epac2 expression in neurons following Epac2-RNAi expression (* $P < 0.001$), $n = 4-8$ cells from 2 experiments. **(c)** Western blot showing RNAi-mediated knockdown of endogenous Epac2 protein in cultured cortical neurons. RNAi plasmid was delivered by nucleofection. **(d)** Effect of 8-CPT treatment on cortical neuron linear density in presence or absence of Epac2 RNAi; spines/10mm: control, 5.04 ± 0.36 ; 8-CPT, 4.28 ± 0.21 , Epac2 RNAi, 5.11 ± 0.34 , Epac2 RNAi+8-CPT, 4.8 ± 0.26 , Epac2 RNAi+Epac2 Rescue, 5.65 ± 0.24 , $P > 0.05$, $n = 5-10$ cells per condition, 3 experiments. **(e)** Effect of SKF-38393 treatment on cortical neuron linear density in presence or absence of Epac2 RNAi, spines/10mm: control, 4.3 ± 0.36 ; SKF-38393, 4.7 ± 0.2 ; Epac2 RNAi 4.7 ± 0.45 ; Epac2 RNAi+SKF-38393 4.4 ± 0.27 , $P > 0.05$, $n = 9-13$ cells per condition, 4 experiments. **(f)** Effects on spine morphology of Epac2 overexpression, as compared to GFP-only controls. **(g)** Quantification of the effects on spine area in d, $n = 7-11$ cells per condition, from 3 experiments. Scale bar, 35μ m.



Supplementary Figure 7 Quantification of the effects of Epac2 activation on synapse and spine remodeling in neurons. **(a)** Quantification of the effect of 8-CPT on spine morphology. Average length, breadth, and breadth/length ratio, in control and 8-CPT-treated neurons were quantified (area (μm^2): control, 0.91 ± 0.03 ; 8-CPT, 0.76 ± 0.02 ; length (μm): control, 2.00 ± 0.04 ; 8-CPT, 2.06 ± 0.05 ; breadth (μm): control, 1.02 ± 0.02 ; 8-CPT, 0.92 ± 0.02 ; breadth/length: control, 0.55 ± 0.01 ; 8-CPT, 0.49 ± 0.01 , $*P < 0.001$, $n = 391$ -446 spines, 14-16 cells per condition, 4 experiments). **(b)** Lack of effect of 8-CPT (50 μM , 1 hr) on spine density: spines/10 μm : control, 5.58 ± 0.22 ; 8-CPT, 5.59 ± 0.44 , $P > 0.05$, $n = 14$ -16 cells per condition, 4 experiments. **(c)** Expression of dominant-negative Rap1 and Rap2 (Rap1-DN, Rap2-DN) prevents 8-CPT-induced spine remodeling, $*P < 0.01$, $n = 212$ -276 spines, 4-8 cells per condition, 3 experiments. **(d)** Activation of endogenous Epac2 by incubating GFP-expressing cultured cortical pyramidal neurons (div 28) with 8-CPT (50 μM , 1 hr) induces spine remodeling and alters spine/bassoon overlap. **(e)** Quantification of the effect of incubation with 8-CPT on presynaptic terminals. Average area, integrated intensity, and average intensity of total bassoon immunofluorescence in control and 8-CPT-treated neurons were quantified. $n = 5$ -7 cells per condition, 2 experiments. **(f)** 8-CPT treatment reduces bassoon-spine overlap; bassoon immunofluorescence (a.u.): control, 7.00 ± 0.21 ; 8-CPT, 5.72 ± 0.22 , $*P < 0.001$, $n = 6$ cells per condition, 2 experiments. The effect of 8-CPT on bassoon overlap is blocked by Epac2 RNAi; (a.u.) Epac2 RNAi, 5.78 ± 0.18 ; RNAi+8-CPT, 5.74 ± 0.17 , $n = 11$ -12 cells per condition, 2 experiments. **(g)** Quantification of the effect of incubation with 8-CPT on average intensity of bassoon immunofluorescence overlapping with GluR2/3, $n = 14$ -17 cells per condition, 3 experiments. **(h)** Quantification of the effect of 8-CPT on percent GluR2/3 overlap with bassoon (Fig. 3e). Scale bar, 5 μm .



Supplementary Figure 8 Time-lapse imaging of spine dynamics. **(a)** Control or 8-CPT pre-treated cells were imaged at 10-min intervals for up to 80 minutes; selected frames are shown. Arrowheads, spine turnover. **(b)** Quantification of spine motility, expressed separately as spines undergoing extension, retraction or head morphing, * $P < 0.001$ $n = 1218$ spines from 5 cells per condition; total spine motility is shown in Fig. 2f. **(c)** 8-CPT fails to increase spine motility in Epac2-RNAi-treated neurons **(d)** Quantification of c, normalized total motility: Epac2 RNAi, 0.16 ± 0.03 ; Epac2 RNAi+8-CPT, 0.19 ± 0.03 , $P > 0.05$. **(e)** Detailed motility quantification of c. **(f)** Spine shrinkage was not caused by photodamage, as spines in vehicle-treated neurons were stable over 120 min of imaging. Scale bars: a, c, 5 μm ; f, 2.5 μm .

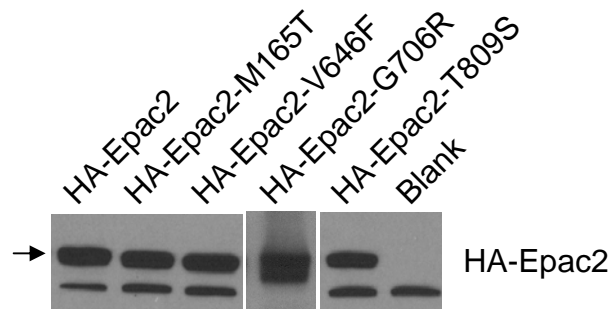


Supplementary Figure 9 Interaction of Epac2 with NL3. **(a)** Incubation of pyramidal neurons (div 28) with 8-CPT (50 mM) increases the interaction of Epac2 with NL3, as shown by coimmunoprecipitation, $n = 2$ experiments, Western Blot shows representative results. **(b)** Coimmunoprecipitation of exogenous Epac2 with NL3 or PSD-95 from hEK293 cells. Cells were transfected with plasmids expressing HA-Epac2, alone or with GFP-NL3 or PSD-95, and immunoprecipitated with HA antibody. **(c)** Expression of GFP-NL3 affects endogenous Epac2 subcellular localization in dendrites. Line scans through dendrites and spines (yellow lines) to visualize Epac2 distribution across the dendrite. **(d)** Plots of lines scans of Epac2 immunofluorescence intensities from lines scans similar to those in c. In the absence of GFP-NL3, endogenous Epac2 is diffuse throughout the cell; in the presence of GFP-NL3, endogenous Epac2 has a greater membrane localization. **(e)** Quantification of the effect of 8-CPT on Epac2 and NL3 colocalization and puncta counts (data shown in Fig. 6f). 8-CPT treatment increased Epac2 puncta number but did not affect NL3 puncta: Epac2: control, 7.69 ± 0.21 ; 8-CPT, 11.52 ± 0.58 . NL3: control, 8.09 ± 1.43 ; 8-CPT, 8.60 ± 0.48 . Intensities of Epac2 clusters were averaged for each point, $n = 10$ cells per condition, 2 experiments.

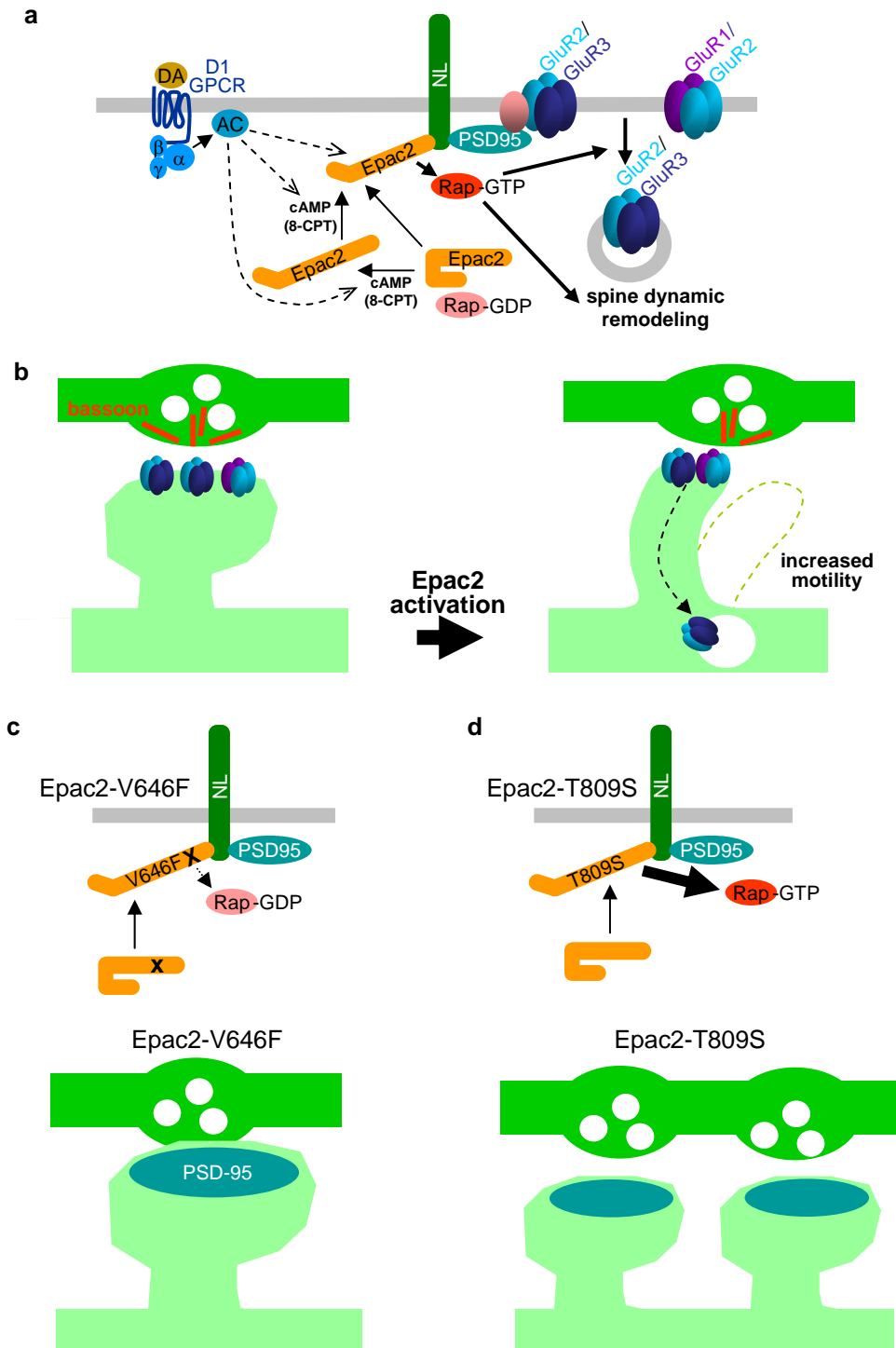
a



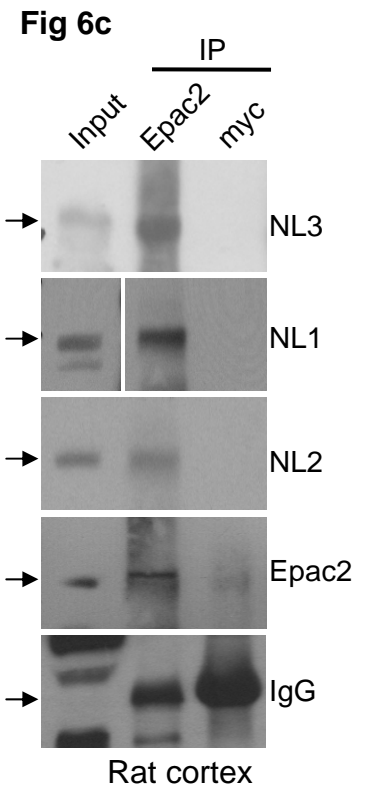
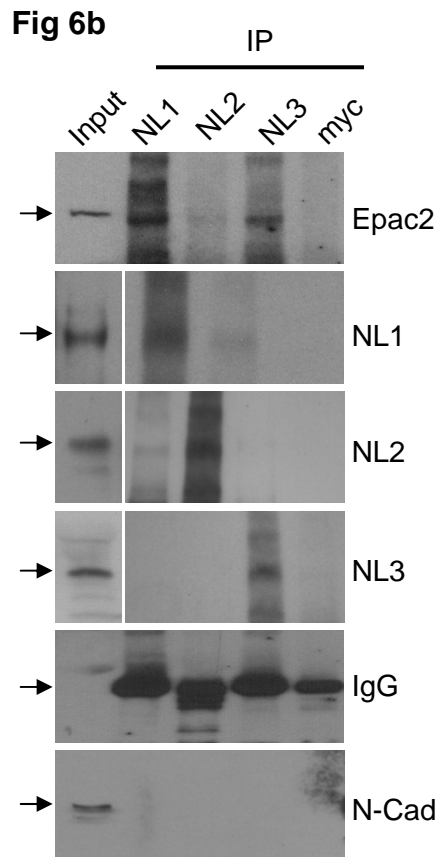
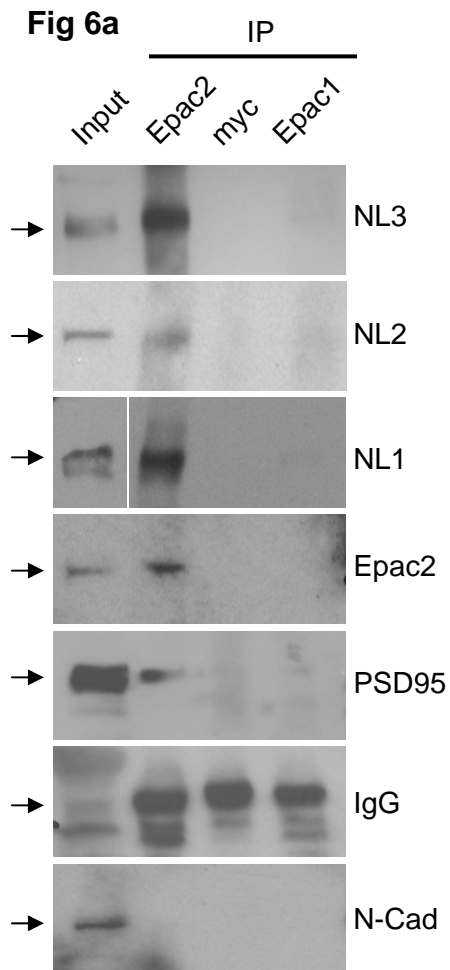
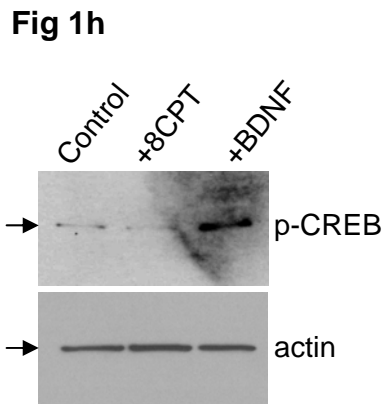
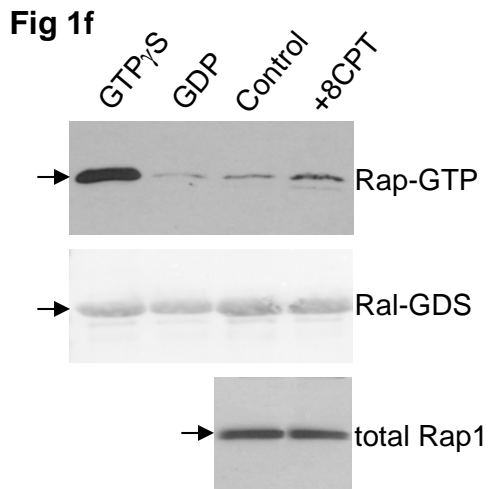
b



Supplementary Figure 10 Disease-associated variants of Epac2. **(a)** Domain structure of Epac2; asterisks (*) indicate autism-associated mutations. **(b)** HA-tagged Epac2 mutants express normally in hEK293 cells.



Supplementary Figure 11 Model of synapse dynamic remodeling regulated by Epac2. **(a)** Binding of cAMP produced upon D1-like dopamine receptor activation (mimicked by 8-CPT), or recruitment to the plasma membrane by NL3, enhance Epac2 Rap-GEF activity, leading to spine dynamic remodeling and removal of GluR2/3-containing AMPARs. **(b)** Epac2-dependent Rap activation promotes spine shrinkage, motility, and synaptic depression. **(c)** The Epac2-V646F mutation reduces Rap-GEF activity and dendritic Rap signaling, leading to spine enlargement. **(d)** The Epac2-T809S mutation increases NL3-dependent enhancement of Rap-GEF activity, dendritic Rap signaling, leading to increased spine numbers.



Supplementary Figure 12. Uncropped western blots from Fig 1 and Fig 6.

Fig 6h

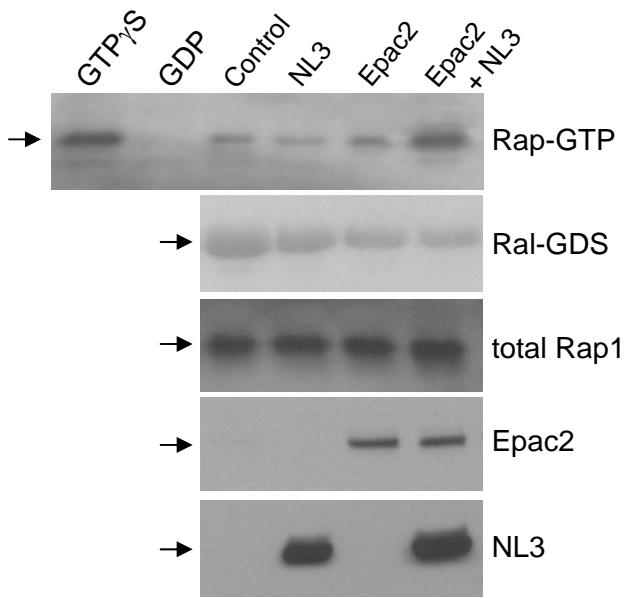


Fig 7a

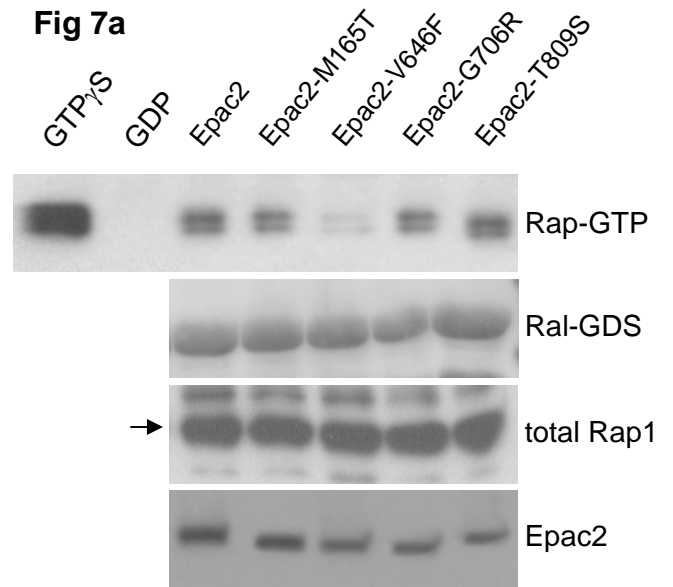
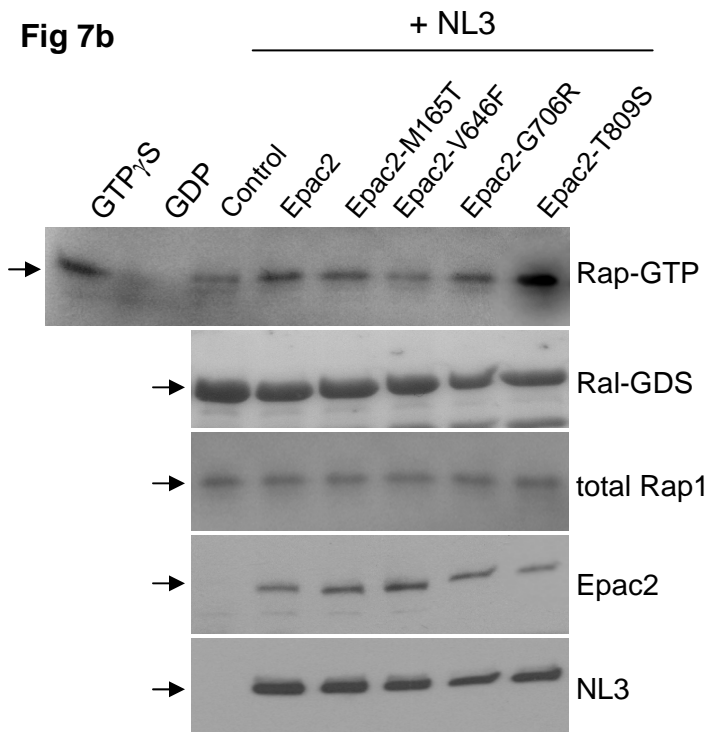


Fig 7b



Supplementary Figure 13. Uncropped western blots from Fig 6 and Fig 7.

Supplementary Table 1. Sequences of primers used in RT-PCR experiments.

Gene	Primer Sequence	Amplicon	GenBank Accession Number
<i>EPAC1</i>	forw: 5' AACTAGCTGCTGTTCTGCTC 3'	85 nt	NM_021690
	rev: 5' TACCATGAGGTACCCTTGTC 3'		
<i>EPAC2</i>	forw: 5' CAAGAGACACCTCCTGAGAG 3'	110 nt	XM_001060956
	rev: 5' CTGATGGTTCCTAAGCTACG 3'		
<i>Rpl19</i>	forw: 5'GTCAACAGATCAGGAAGCTG 3'	138 nt	NM_031103
	rev: 5' TACCCTTCCTCTTCCCTATG 3'		

Supplementary Table 2. Sequences used to generate Epac2 disease-associated point mutations.

Epac2 mutation	Primer sequence
Epac2-M165T	5'- cctccctatggtgta C ggaaacgggctctaac -3'
Epac2-V646F	5'- cacagaagaagcacaag T gcttttgcaacagttc -3'
Epac2-G706R	5'- caaactgggctca A gggaaggcctgat -3'
Epac2-T809S	5'- ggaaggcataattttaaaaga G cacggcaaactggattgttc -3'

SUPPLEMENTARY RESULTS

Epac2 in dendrites and spines

Epac2 colocalized with the dendritic markers Map2 indicating dendritic presence (Supplementary Fig. 2a-b), and at higher magnification, Epac2 puncta were offset from the dendrite shaft, suggesting synaptic presence (Supplementary Fig. S2c). In addition to being enriched in synapses, Epac2 immunofluorescence was also present in small punctate structures in dendritic shafts (“d” in Supplementary Fig. 2d). Epac2 was present in the soma (“s”), indicating a somatodendritic presence. In synapses, Epac2 immunoreactivity partially overlapped with bassoon (Supplementary Fig. 2e). Similar results were obtained with additional commercial Epac2 antibodies. A negative control for antibody staining, lacking primary antibody, confirmed the specificity of the primary antibody (Supplementary Fig. 2f). We analyzed colocalization of Epac2 immunofluorescence with the axonal marker tau (Supplementary Fig. 2g). We found that small amounts of Epac2 immunofluorescence colocalized with tau (white arrows), indicating presence in axons. Occasional Epac2 positive puncta are present in segments in between dendrites of neighboring neurons. However, there were numerous presynaptic boutons without Epac2 (red arrows).

Treatments with 8-CPT

To confirm the specificity of Epac2 activation by 8-CPT in a cellular system, we examined the direct regulation of Epac2 GEF activity by 8-CPT in transfected hEK293 cells, and quantified activation of endogenous Rap by measuring the

amount of Rap1-GTP bound to RalGDS affinity resin and Western blotting (Supplementary Fig. 3a-b). Incubation with 10 μ M 8-CPT enhanced Rap activation in cells expressing exogenous Epac2 (2.58 ± 1.08 fold increase vs. untreated controls). Activation did not occur when a mutant Epac2 lacking the Rap-GEF domain (Epac2- Δ GEF) was expressed, demonstrating that 8-CPT enhanced the Rap-GEF activity of Epac, and thus can be used to specifically activate Epac2 in neurons. To further confirm the PKA-independence of 8-CPT-induced Rap activation in neurons, we incubated neurons with 2-100 μ M 8-CPT, alone or in presence of the PKA inhibitor peptide (PKI-(Myr-14-22)-amide) (data not shown). Increasing concentrations of 8-CPT resulted in increased levels of active Rap, which were not blocked by PKI, indicating that PKA did not contribute to the 8-CPT-induced Rap activation. As in non-neuronal cells, 8-CPT incubation also activated Rap2 (Supplementary Fig. 3c).

RNA interference

We first tested the effectiveness of knockdown of Epac2 in heterologous cells and neurons. RNAi effectively knocked down the expression of exogenous epitope-tagged Epac2 in hEK293 cells (Supplementary Fig. 5a), and endogenous Epac2 in primary cortical neurons transfected using nucleofection (Supplementary Fig. 6c), and reduced the expression of exogenous Epac2 protein, but not of an unrelated protein, in cultured neurons (Supplementary Fig. 5c). A rescue Epac2 mutant expressed in neurons (Supplementary Fig. 5c), and was not knocked down by RNAi (Supplementary Fig. 5b). Epac2 RNAi reduced

the expression of endogenous Epac2 protein in cultured neurons (Supplementary Fig. 6a). We quantified the amount of Epac2 RNAi knockdown, after 3 and 5 days, and found that it resulted in ~30% and ~70% knockdown respectively (Supplementary Fig. 6b).

SUPPLEMENTARY DISCUSSION

Specificity of 8-CPT for Epac

8-CPT specifically activates Epac, but not PKA, both *in vitro* and *in vivo*¹, thus it has been used extensively to study Epac². 8-CPT is ~100-fold more selective for Epac vs. PKA, binds Epac 10-fold better than cAMP itself, and activates it 3-fold better than cAMP². Although at concentrations >100 μ M 8-CPT activates both Epac and PKA *in vitro*, in live cells 30-300 μ M 8-CPT did not induce PKA-dependent CREB phosphorylation activation, while application of the same concentrations of PKA-activating cAMP analogs caused CREB activation³. Similarly, we found that in pyramidal neurons 50-100 μ M 8-CPT activated Rap effectively, which was not blocked by PKI and did not cause CREB phosphorylation, indicating that PKA did not have a significant contribution. Importantly, the 8-CPT concentrations used in our study are identical to those used in other cell types, and similar to those required for half maximal activation (AC_{50}) of Epac^{1,3}. Although the affinity (EC_{50}) of cAMP binding to the isolated cAMP-binding domain of Epac is in the low μ M range, the AC_{50} of Epac2 is 10 times higher², in the range of the concentrations used. Hence 8-CPT is a highly selective activator of Epac. Although there is an extensive amount of data

showing that 8-CPT is specific for Epac, as with any pharmacological agent, there is a chance that it may also affect other targets. Because Epac2 is far more abundant than Epac1 in cortical neurons and postsynaptic densities, our observed effects are primarily due to Epac2 activation. Most importantly, the effects of 8-CPT on spine morphology and AMPAR currents were prevented by Epac2 knockdown and Epac- Δ GEF, demonstrating that in cortical pyramidal neurons 8-CPT specifically acts through Epac2 and independently of PKA. It is important to note that incubation of neurons with 8-CPT activates Epac2 throughout the cell. 8-CPT increases the clustering of endogenous Epac2 (Fig. S3d). As 8-CPT acts rapidly on spines and AMPA mEPSCs, the possibility of involvement of gene expression in these processes is unlikely. In addition, we found that 8-CPT effects on spines were not blocked by protein synthesis inhibitors (data not shown).

In principle, there are several possible mechanisms whereby 8-CPT may activate Rap. Activation of Epac1 or Epac2: Epac1 is expressed at very low levels in the investigated neurons, and the effects of 8-CPT on spine morphology, motility, phospho-B-Raf, AMPA receptors, and AMPA mEPSC were prevented by RNAi knockdown of Epac2, demonstrating that they specifically depend on Epac2, and not PKA or other effectors. While 8-CPT was developed to preferentially activate Epac2 over PKA, assuming that 8-CPT may activate PKA to some extent, it may activate Rap through its direct phosphorylation on Ser-179⁴ or through C3G⁵. In PC12 cells cAMP, forskolin, or 8-CPT activated the Rap1-B-Raf-Elk-1 pathway, likely through PKA-dependent phosphorylation of

Rap1 at Ser-179^{4,6}. cAMP activated a membrane associated pool of Rap, leading to ERK activation, through the RapGEF C3G. As this GEF does not directly bind cAMP, it is unlikely that it directly binds 8-CPT. In cerebellar granule cells, Obara et al.⁷ found that Rap1 was activated by cAMP, PACAP, and KCl via PKA-dependent mechanisms, and that this cAMP-activated Rap1 participated in the activation of a selective membrane-associated pool of ERK. However, the main mechanism of ERK activation was through cAMP, PACAP, KCl, and BDNF and Ras, and required PKA⁷. Rap1 activation by PKA required Src family kinases. In primary neurons, the PKA requirement of cAMP activation of ERKs appears to be neuronal cell-type dependent⁷. In cortical neurons, cAMP activation of ERKs has both a PKA-dependent and PKA-independent component⁸. In hippocampal neurons, the requirement of PKA in cAMP's activation of ERKs has not been examined. Zhong and Zucker⁹ have shown that 8-CPT does not activate HCN channels. Moreover, HCN channels have not been linked to either Rap activation or spine remodeling. The existence of unknown effectors of 8-CPT, as well as non-specific effects, are not completely impossible, as with any pharmacological agent. However, extensive characterization of 8-CPT, as well as our RNAi controls, show that the effects of 8-CPT on spines are Epac2-dependent.

Rap is activated by Rap-GEFs or by inhibition of Rap-GAPs. The only known Rap-GEFs that directly bind cAMP are Epac1 and 2. PDZ-GEF1 (or cNRasGEF) has been shown by some studies to activate Ras and Rap in response to cAMP and cGMP¹⁰. However, another study using affinity

measurements by isothermic calorimetry found that PDZ-GEF1 does not bind cAMP with a physiologically relevant affinity, and is not responsive to cAMP and various other nucleotides¹¹. Binding to 8-CPT has not been examined in either study. Whereas two RapGEFs, RapGEF2 and 6 (PDZ-GEFs 1 and 2) have putative cAMP binding domains, they lack key residues for nucleotide binding and do not associate with cAMP¹¹. Another possibility is that cAMP activates Ras, and then Ras activates Epac2 in conjunction with cAMP, as shown by Li et al., 2006 and Liu et al., 2008^{12,13}.

Spine shrinkage vs. elimination

Though spine shrinkage and spine elimination are related concepts, the former does not necessarily result in the later. Epac2 activation did not reduce spine density, but promoted spine shrinkage and reduced pre-postsynaptic contact. Notably, reduced pre and postsynaptic apposition without spine elimination has also been observed in living slices under LTD-inducing conditions¹⁴. Few molecules, when activated, are known to promote spine shrinkage without elimination, and we have previously shown that Rap1 is one of these molecules¹⁵.

Presynaptic vs. postsynaptic Epac2 signaling

Our data indicate that a significant amount of Epac2 is present postsynaptically. Knockdown of Epac2 using RNAi demonstrates a postsynaptic role for this protein in regulating 8-CPT- and DAR-D1/D5-dependent control of dendritic spine

morphology and GluR2/3 trafficking. However, we also observed Epac2 immunofluorescence in small puncta along axons, and detected a reduction in mEPSC frequency following treatment with 8-CPT that was not blocked by postsynaptic knockdown of Epac2. These data are indicative of some presynaptic presence and function of Epac2 in mature cortical neurons.

Dopamine signaling

While numerous studies indicate a role of D1/D5 receptors in potentiation (such as Smith et al., ¹⁶), a large number of studies indicate a role in synaptic depression ¹⁷⁻²⁵. The determinants of this directionality have not yet been extensively explored, but seem to be affected by the neuronal type, brain region, age, or method of stimulation. Smith et al. ¹⁶ used hippocampal neurons (div 14-21) incubated with SKF-38393 (100 μ M) and dihydrexidine (DHX) to show that SKF-38393/DHX increase local protein synthesis in a PKA-dependent manner. They see increased GluR1 at the surface after 15 min DHX, which was local protein synthesis-dependent, and found that DHX increases mEPSC frequency, but has no effect on amplitude. These effects were blocked by PKA and by inhibiting local protein synthesis. On the other hand, we examined div 28 cortical neurons, and the effects we observed were not PKA- and protein-synthesis dependent, and were blocked by Epac2 RNAi. In support of this, we show that SKF-38393 also stimulated phosphorylation of B-Raf, a known Rap substrate, in an Epac2-dependent manner (Fig. 5c-d).

Interestingly, recent studies found potential links between dopamine and cAMP signaling and the autistic phenotype. Genetic studies found associations of autism with dopamine signaling, including D1 and D3 receptors, which modulate cAMP, and DAT1 dopamine transporter²⁶⁻²⁸. Moreover, alterations in cAMP signaling have been found in fragile-X, a disorder with significant comorbidity with autism, and the fragile X-mental retardation protein FMRP has been identified as a key messenger for dopamine modulation²⁹⁻³¹. The detailed mechanisms are not yet understood, but these new findings clearly implicate dopamine and cAMP signaling in autism and related disorders.

Potential disease association

It is of note that the chromosomal region that includes Epac2 (2q31-q32) has been implicated in ASD by multiple studies. Several independent genome-wide linkage studies identified the 2q chromosomal region as an autism susceptibility locus³²⁻³⁴, and a genome-wide screen performed by IMGSAAC yielded the 2q21-33 region as the most significant (MLS score of 3.74)³⁵. A 2q31-32 de novo deletion has also been reported in a high-functioning autistic individual³⁶.

Another independent study found association of 2q31.1 with autism in 143 Sicilian (Italian) TRIO families³⁷. Interestingly, a genome-wide linkage scan identified chromosomal region 2q24.1-31.1 as a significant (LOD score 4.42) quantitative-trait locus for IQ³⁸. These genetic studies suggest that a gene or genes associated with autism and cognitive development are located in this region³⁹. However, the mutations in Epac2 do not account for this association,

as they are rare. Rare mutations have been recently implicated in psychiatric disorders, suggesting that a significant fraction of cases may be caused by rare mutations ⁴⁰.

Defective synapse remodeling is thought to contribute to autism ^{41,42}. In addition, brain circuit miswiring has been proposed to contribute to ASD ⁴³, and synaptic dysfunction could be an important contributor to this. This hypothesis is also supported by the modulatory effect of several autism-associated proteins (including NLs and shank3) on spine morphology ⁴⁴⁻⁴⁶. Postmortem neuropathological studies found alterations of dendritic spine morphology in patients with ASD ⁴⁷ and in patients with other diseases with comorbidity with autism, including Rett syndrome, fragile-X, tuberous sclerosis ^{48,49}, supporting a role for altered synapse remodeling in the autistic phenotype.

SUPPLEMENTARY REFERENCES

1. Enserink, J.M. et al. A novel Epac-specific cAMP analogue demonstrates independent regulation of Rap1 and ERK. *Nat Cell Biol* **4**, 901-906 (2002).
2. Bos, J.L. Epac proteins: multi-purpose cAMP targets. *Trends Biochem Sci* **31**, 680-686 (2006).
3. Kang, G. et al. Epac-selective cAMP analog 8-pCPT-2'-O-Me-cAMP as a stimulus for Ca²⁺-induced Ca²⁺ release and exocytosis in pancreatic beta-cells. *J Biol Chem* **278**, 8279-8285 (2003).
4. Vossler, M.R. et al. cAMP activates MAP kinase and Elk-1 through a B-Raf- and Rap1-dependent pathway. *Cell* **89**, 73-82 (1997).
5. Wang, Z. et al. Rap1-mediated activation of extracellular signal-regulated kinases by cyclic AMP is dependent on the mode of Rap1 activation. *Mol Cell Biol* **26**, 2130-45 (2006).
6. York, R.D. et al. Rap1 mediates sustained MAP kinase activation induced by nerve growth factor. *Nature* **392**, 622-6 (1998).
7. Obara, Y., Horgan, A.M. & Stork, P.J. The requirement of Ras and Rap1 for the activation of ERKs by cAMP, PACAP, and KCl in cerebellar granule cells. *J Neurochem* **101**, 470-82 (2007).
8. Ambrosini, A. et al. cAMP cascade leads to Ras activation in cortical neurons. *Brain Res Mol Brain Res* **75**, 54-60 (2000).
9. Zhong, N. & Zucker, R.S. cAMP acts on exchange protein activated by cAMP/cAMP-regulated guanine nucleotide exchange protein to regulate transmitter release at the crayfish neuromuscular junction. *J Neurosci* **25**, 208-214 (2005).
10. Pham, N. et al. The guanine nucleotide exchange factor CNrasGEF activates ras in response to cAMP and cGMP. *Curr Biol* **10**, 555-8 (2000).
11. Kuiperij, H.B. et al. Characterisation of PDZ-GEFs, a family of guanine nucleotide exchange factors specific for Rap1 and Rap2. *Biochim Biophys Acta* **1593**, 141-9 (2003).
12. Li, Y. et al. The RAP1 guanine nucleotide exchange factor Epac2 couples cyclic AMP and Ras signals at the plasma membrane. *J Biol Chem* **281**, 2506-2514 (2006).
13. Liu, C. et al. Ras is required for the cyclic AMP-dependent activation of Rap1 via Epac2. *Mol Cell Biol* **28**, 7109-25 (2008).

14. Bastrikova, N., Gardner, G.A., Reece, J.M., Jeromin, A. & Dudek, S.M. Synapse elimination accompanies functional plasticity in hippocampal neurons. *Proc Natl Acad Sci U S A* **105**, 3123-7 (2008).
15. Xie, Z., Huganir, R.L. & Penzes, P. Activity-dependent dendritic spine structural plasticity is regulated by small GTPase Rap1 and its target AF-6. *Neuron* **48**, 605-618 (2005).
16. Smith, W.B., Starck, S.R., Roberts, R.W. & Schuman, E.M. Dopaminergic stimulation of local protein synthesis enhances surface expression of GluR1 and synaptic transmission in hippocampal neurons. *Neuron* **45**, 765-79 (2005).
17. Calabresi, P. et al. Dopamine and cAMP-regulated phosphoprotein 32 kDa controls both striatal long-term depression and long-term potentiation, opposing forms of synaptic plasticity. *J Neurosci* **20**, 8443-51 (2000).
18. Calabresi, P., Maj, R., Mercuri, N.B. & Bernardi, G. Coactivation of D1 and D2 dopamine receptors is required for long-term synaptic depression in the striatum. *Neurosci Lett* **142**, 95-9 (1992).
19. Chen, Z. et al. Activation of dopamine D1 receptors enhances long-term depression of synaptic transmission induced by low frequency stimulation in rat hippocampal CA1 neurons. *Neurosci Lett* **188**, 195-8 (1995).
20. Chen, Z. et al. Roles of dopamine receptors in long-term depression: enhancement via D1 receptors and inhibition via D2 receptors. *Receptors Channels* **4**, 1-8 (1996).
21. Huang, Y.Y., Simpson, E., Kellendonk, C. & Kandel, E.R. Genetic evidence for the bidirectional modulation of synaptic plasticity in the prefrontal cortex by D1 receptors. *Proc Natl Acad Sci U S A* **101**, 3236-3241 (2004).
22. Lemon, N. & Manahan-Vaughan, D. Dopamine D1/D5 receptors gate the acquisition of novel information through hippocampal long-term potentiation and long-term depression. *J Neurosci* **26**, 7723-9 (2006).
23. Otani, S., Blond, O., Desce, J.M. & Crepel, F. Dopamine facilitates long-term depression of glutamatergic transmission in rat prefrontal cortex. *Neuroscience* **85**, 669-76 (1998).
24. Shen, W., Flajolet, M., Greengard, P. & Surmeier, D.J. Dichotomous dopaminergic control of striatal synaptic plasticity. *Science* **321**, 848-51 (2008).
25. Zhang, Y., Deng, P., Ruan, Y. & Xu, Z.C. Dopamine D1-like receptors depress excitatory synaptic transmissions in striatal neurons after transient forebrain ischemia. *Stroke* **39**, 2370-6 (2008).

26. de Krom, M. et al. A common variant in DRD3 receptor is associated with autism spectrum disorder. *Biol Psychiatry* **65**, 625-30 (2009).
27. Gadow, K.D., Roohi, J., DeVincent, C.J. & Hatchwell, E. Association of ADHD, tics, and anxiety with dopamine transporter (DAT1) genotype in autism spectrum disorder. *J Child Psychol Psychiatry* **49**, 1331-8 (2008).
28. Hettinger, J.A., Liu, X., Schwartz, C.E., Michaelis, R.C. & Holden, J.J. A DRD1 haplotype is associated with risk for autism spectrum disorders in male-only affected sib-pair families. *Am J Med Genet B Neuropsychiatr Genet* **147B**, 628-36 (2008).
29. Kelley, D.J. et al. The cyclic AMP phenotype of fragile X and autism. *Neurosci Biobehav Rev* **32**, 1533-43 (2008).
30. Kelley, D.J. et al. The Cyclic AMP Cascade Is Altered in the Fragile X Nervous System. *PLoS ONE* **2**, e931 (2007).
31. Wang, H. et al. FMRP acts as a key messenger for dopamine modulation in the forebrain. *Neuron* **59**, 634-47 (2008).
32. Buxbaum, J.D. et al. Evidence for a susceptibility gene for autism on chromosome 2 and for genetic heterogeneity. *Am J Hum Genet* **68**, 1514-20 (2001).
33. Philippe, A. et al. Genome-wide scan for autism susceptibility genes. Paris Autism Research International Sibpair Study. *Hum Mol Genet* **8**, 805-12 (1999).
34. Shao, Y. et al. Phenotypic homogeneity provides increased support for linkage on chromosome 2 in autistic disorder. *Am J Hum Genet* **70**, 1058-61 (2002).
35. A genomewide screen for autism: strong evidence for linkage to chromosomes 2q, 7q, and 16p. *Am J Hum Genet* **69**, 570-81 (2001).
36. Gallagher, L. et al. Brief report: A case of autism associated with del(2)(q32.1q32.2) or (q32.2q32.3). *J Autism Dev Disord* **33**, 105-8 (2003).
37. Romano, V. et al. Suggestive evidence for association of D2S2188 marker (2q31.1) with autism in 143 Sicilian (Italian) TRIO families. *Psychiatr Genet* **15**, 149-50 (2005).
38. Posthuma, D. et al. A genomewide scan for intelligence identifies quantitative trait loci on 2q and 6p. *Am J Hum Genet* **77**, 318-26 (2005).
39. Persico, A.M. & Bourgeron, T. Searching for ways out of the autism maze: genetic, epigenetic and environmental clues. *Trends Neurosci* **29**, 349-58 (2006).
40. Walsh, T. et al. Rare structural variants disrupt multiple genes in neurodevelopmental pathways in schizophrenia. *Science* **320**, 539-43 (2008).

41. Ramocki, M.B. & Zoghbi, H.Y. Failure of neuronal homeostasis results in common neuropsychiatric phenotypes. *Nature* **455**, 912-8 (2008).
42. Zoghbi, H.Y. Postnatal neurodevelopmental disorders: meeting at the synapse? *Science* **302**, 826-30 (2003).
43. Geschwind, D.H. Autism: many genes, common pathways? *Cell* **135**, 391-5 (2008).
44. Chih, B., Afridi, S.K., Clark, L. & Scheiffele, P. Disorder-associated mutations lead to functional inactivation of neuroligins. *Hum Mol Genet* **13**, 1471-7 (2004).
45. Durand, C.M. et al. Mutations in the gene encoding the synaptic scaffolding protein SHANK3 are associated with autism spectrum disorders. *Nat Genet* **39**, 25-7 (2007).
46. Tabuchi, K. et al. A neuroligin-3 mutation implicated in autism increases inhibitory synaptic transmission in mice. *Science* **318**, 71-6 (2007).
47. Pickett, J. & London, E. The neuropathology of autism: a review. *J Neuropathol Exp Neurol* **64**, 925-935 (2005).
48. Armstrong, D.D. Neuropathology of Rett syndrome. *J Child Neurol* **20**, 747-53 (2005).
49. Irwin, S.A., Galvez, R. & Greenough, W.T. Dendritic spine structural anomalies in fragile-X mental retardation syndrome. *Cereb Cortex* **10**, 1038-44 (2000).